Self-Assembly of *n*-Alkanethiol Monolayers. A Study by IR−Visible Sum Frequency Spectroscopy (SFG)

M. Himmelhaus, F. Eisert, M. Buck,* and M. Grunze

Lehrstuhl für Angewandte Physikalische Chemie, Universität Heidelberg, Im Neuenheimer Feld 253, 69120 Heidelberg, Germany

Received: June 22, 1999; In Final Form: October 21, 1999

Adsorption of docosanethiol ($CH_3(CH_2)_{21}SH$) onto polycrystalline gold from ethanol solution was investigated by nonlinear vibrational spectroscopy. The formation of the self-assembled monolayer (SAM) was monitored by recording of the temporal evolution of the C−H stretching modes. Three different steps with significantly different time scales were identified. The fastest step in the adsorption process is related to the Au−S bond formation. Progressing with a rate constant of 2500−3000 L mol^{-1} s^{-1}, it is characterized by hydrocarbon chains with a high fraction of gauche kinks. The second step proceeds 3−4 times more slowly and comprises the straightening of the alkane chains. During the first two steps a pronounced band around 2813 cm^{-1} appears, which is interpreted as mode softening of the C−H vibrations due to the interaction with the substrate. The time scale of the final step is a factor of 35−70 slower than the rate of chain stretching and encompasses the reorientation of the terminal methyl end groups. The methylene group adjacent to the methyl group exhibits the same temporal behavior and thus behaves oppositely to the other methylene groups. The SFG data imply that the last few percent of the thiol molecules adsorbing produce the complete monolayer by inducing the transition from a high number of gauche defects to an all-trans conformation. The sequence of changes in the vibrational spectra suggests an ordering and annealing of the film from the interface to the film surface.

I. Introduction

The mechanism of self-assembly of *n*-alkanethiols on gold surfaces has been the focus of a number of studies over the past decade, and there is general agreement that formation of thiol SAMs occurs stepwise. The first kinetic study of thiol adsorption from solution using ellipsometry and contact angle measurements revealed a two-step process: a first fast step during which most of the thiol adsorption occurs and a second, significantly delayed step which yields the final monolayer.[1] This two-step process was later confirmed and detailed by combining in situ investigations of the thiol adsorption by second harmonic generation (SHG) and the ex situ characterization by near-edge X-ray absorption fine structure spectroscopy (NEXAFS).[2−4] During the first step the thiol coverage quickly increases up to a coverage of about 80−90% of the completed monolayer. The increase in coverage up to the final value was identified to take place much more slowly in a second step. During this period of time the hydrocarbon chains undergo a transition from a high degree of gauche defects to an all-trans conformation. Following this early investigations other techniques such as quartz crystal microbalance (QCM),[5] IR reflection absorption spectroscopy (IRRAS),[6,7] and surface plasmon spectroscopy[8,9] were applied to elucidate the mechanism in more detail. The majority of investigations agree that there is a fast initial step during which most of the thiols are adsorbed. As revealed by scanning probe microscopies[10,11] and SHG,[12] coverage increases via island formation. The in situ SHG experiments also indicated that displacement of solvent molecules or contamination from the surface is rate-limiting.[12] However, the steps following the initial fast one are much less clear. This is partly due to the fact that most of the techniques applied measure indirect quantities such as mass loading or index of refraction rather than providing direct information about the orientation of molecular entities or the molecular conformation.

Similarly to investigations on film formation from solution, mechanistic studies under UHV conditions using low-energy electron diffraction (LEED),[13,14] He scattering, X-ray based techniques,[15,16] and scanning tunneling microscopy[17] also revealed a stepwise mechanism. A striped phase with the molecules lying down forms initially and transforms to the c(4 × 2) structure at high coverage. Between these structurally well-defined phases another phase emerges at intermediate coverage, which is disordered and does not show He atom or X-ray diffraction.[16]

Contrary to the detailed UHV studies of thiol adsorption from the gas phase, the mechanistic details of film formation by adsorption from solution are less clear. This is partly due to the techniques used which yield only indirect information such as changes of the index of refraction or mass loading. Techniques such as vibrational spectroscopies or NEXAFS, which can provide more detailed molecular information, have been applied in a few cases only.[2,6,7] At present it is not clear how well the scheme of film formation developed for UHV conditions can be transferred to the standard preparation conditions for solutions. In particular, it can be expected that the solvent interacts with the thiol molecules and the substrate and thus takes part in the process of film formation.

For the investigation of thiol SAMs formed by adsorption from solution, we applied IR−vis sum frequency generation (SFG), a technique which provides very specific information about the system via the molecular vibrations. This ex situ study continues our work on the mechanism of film formation and focuses on the adsorption stages after the initial fast adsorption step which has been studied in detail by in situ second harmonic generation.[12]

10.1021/jp992073e CCC: $19.00
Published on Web 12/29/1999

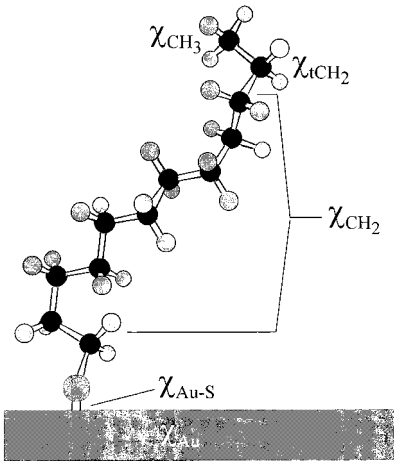

Figure 1. Illustration of the different susceptibilities of a thiol molecule adsorbed on gold. The sum frequency signal is determined by a coherent superposition of nonresonant (χ_{Au}, χ_{Au-S}) and resonant contributions (χ_{CH_3}, χ_{CH_2}, χ_{tCH_2}). The terminal CH_2 group differs from the other methylene moieties.

SFG has demonstrated to be a powerful technique for studying ultrathin organic films[18−20] since it combines several advantages. First, as a photon-based technique SFG is not restricted to vacuum. Second, being a second-order process it is sensitive to breaking of inversion symmetry, which is not only the basis of its interface sensitivity but also makes it sensitive to the conformation of alkane chains. Third, due to its high interface sensitivity a reference spectrum is not required, unlike for IR reflection absorption spectroscopy. This important point will be addressed in detail below in conjunction with the role of contaminations in the adsorption kinetics.

In contrast to other interface sensitive techniques such as plasmon spectroscopy, SFG yields very specific information via the molecular vibrations of the adsorbate. SFG also traces the Au−S bond formation, thus providing direct information on the thiol coverage.

The paper is organized such that the theory section presents the basics for the analysis of the spectra. SFG with IR spectra from completed SAMs of docosanethiol are compared to demonstrate the complementarity of both techniques. Subsequently, we give a detailed analysis of the temporal evolution of the vibrational structure for the formation of a SAM of docosanethiol.

II. Theory

The intensity of a sum frequency signal from thiols adsorbed onto a metal substrate is phenomenologically described by a coherent superposition of different contributions.

$$I_{SFG} \propto |\chi_{Au}(\omega) + \chi_{Au-S}(\omega,\theta) + \sum_{\nu}\chi_{\nu}^{CH_n}(\omega,\theta)|^2 I_{vis} I_{IR} \quad (1)$$

I_{IR}, I_{vis} denote the intensities of the incident laser beams. As illustrated in Figure 1 the SFG signal is determined by a number of second-order susceptibilities χ which reflect different sites of the system. χ_{Au} represents the susceptibility of the bare substrate and χ_{Au-S} denotes its alteration upon bonding of thiols. As shown below χ_{Au} and χ_{Au-S} are frequency independent in the wavelength range considered here. Consequently, χ_{Au-S} directly reflects the thiol coverage θ if every thiol molecule contributes equally, i.e., the adsorption sites do not interfere electronically. In contrast to optical second harmonic generation where the susceptibilities $\chi_{\nu}^{CH_n}$ of the methylene ($n = 2$) and methyl groups ($n = 3$) are vanishingly small,[4] for IR−vis SFG they become comparable to the contribution of χ_{Au} and χ_{Au-S} by tuning the IR light into resonance with the vibrations. Perturbation theory yields[21,22]

$$\chi_{\nu}^{CH_n} = \frac{A_{\nu}}{\omega_{\nu} - \omega_{IR} + i\Gamma_{\nu}} \quad (2)$$

where ω_{ν} and Γ denote the frequency of the vibration ν and the Lorentzian line width, respectively. The amplitude factor A_{ν} of a CH_n group is a third rank tensor whose components are given by

$$A_{\nu,ijk} = \frac{2\pi}{h} N \langle \sum_{lmn} F_{\nu,ijk}(i\cdot l)(j\cdot m)(k\cdot n) R_{lm}\mu_n \rangle \quad (3)$$

N is the number of thiols adsorbed and the Fresnel factor $F_{\nu,ijk}$ accounts for the linear optics. R_{lm} and μ_n are the Raman and the infrared transition moments. i,j,k denote the Cartesian coordinates of the substrate and l,m,n refer to the coordinate systems of the molecular moieties. The brackets indicate the average over all orientations of a C−H unit. $A_{\nu,ijk}$ is a complex quantity and is affected by the Fresnel factor, which on metals causes a change of $A_{\nu,ijk}$ both in magnitude and phase if, e.g., the considered vibrational mode alters its orientation. For given θ, equations 1−3 can be summarized to

$$I_{SFG} \propto \left| 1 + \sum_{\nu} \frac{|A_{\nu}^{norm}| e^{i\phi_{\nu}}}{\omega_{\nu} - \omega_{IR} + i\Gamma_{\nu}} \right|^2 I_{vis} I_{IR} \quad (4)$$

where the amplitudes of the resonant signals have been normalized to the sum of the two nonresonant susceptibilities. The overall shape of an SFG spectrum is dependent on the phase relations ϕ_{ν} which can give rise to constructive or destructive interference between resonances and between a resonance and the nonresonant terms. For the analysis of the temporal evolution of a thiol SAM, the SFG spectra are decomposed according to eq 4 and the quantity used for the evaluation is the intensity of a band given by

$$I_{\nu} = \int_{-\infty}^{\infty} \left| \frac{A_{\nu}}{\omega_{\nu} - \omega_{IR} + i\Gamma_{\nu}} \right|^2 d\omega_{IR} = \frac{A_{\nu}^2}{\Gamma_{\nu}} \quad (5)$$

Besides the requirement of a simultaneous IR and Raman activity, two additional conditions have to be met for a vibrational mode to be detected by IR−vis SFG. First, since gold substrates are used μ_n must have a component along the substrate normal. This is equivalent to the "surface selection rule" known in linear-IR reflection absorption spectroscopy. Second, the symmetry properties of the susceptibility tensor require the C−H groups not to be arranged centrosymmetrically, that is the susceptibility vanishes for random orientation as well as for an all-trans conformation of a hydrocarbon chain in the case of the CH_2 groups.

III. Experimental Section

Substrate Preparation. Thin films of polycrystalline gold were prepared by thermal evaporation of 1 nm of titanium as adhesion promoter and subsequent deposition of 100 nm of gold of 99.99% purity onto polished single-crystal silicon (100) wafers (Silicon Sense). Evaporation was performed at a pressure of 2×10^{-7} Torr and a deposition rate of 0.5 nm/s.

Chemicals. Docosanethiol and perdeuterated eicosanethiol were synthesized in our laboratory. Pa. grade ethanol (Riedel-de Häen) and deuterated ethanol (Cambridge Isotope Laboratories) were used as received.

Preparation of Self-Assembled Monolayers. Immediately after removal from the evaporation chamber the Si wafers were cut into pieces of 15 × 20 mm^2 and were dipped into 50 mL of a 3 μM docosanethiol solution for different periods of time. Each sample was exposed individually to a freshly prepared docosanethiol solution in analytical grade ethanol, thus keeping the change of molarity upon adsorption less than 2%. Samples that were not immersed immediately after cutting were stored under pure Argon and always used within 15 min. The overall exposure time to the ambient for all samples before immersion was less than 5 min. Immersion times were varied between 1.5 min and 48 h. After removal from the thiol solution, the samples were rinsed with pure ethanol, blown dry with pure nitrogen, and stored under pure argon or nitrogen.

Perdeuterated thiol SAMs used as reference in the IR experiments and as a control for the SFG spectra were prepared by immersing freshly evaporated Au samples into 20 μM ethanolic solution of perdeuterated eicosanethiol for 24 h.

For the investigation of the nonresonant substrate SFG signal due to increasing adsorption of the docosanethiolate, fresh Au samples were mounted into a sample holder in such a way that they could be immersed into the 3 μM docosanethiolate solution, rinsed with ethanol, and blown dry with nitrogen without detuning the optical setup.

In addition to the spectroscopic characterization by SFG, the sample quality was controlled by X-ray photoelectron spectroscopy (XPS) and IR reflection absorption spectroscopy (IRRAS). XP spectra and IR spectra were acquired with a Leybold Heraeus Max 200 system and a Biorad 175C FTIR spectrometer, respectively.

Sum Frequency Spectroscopy (SFG). IR−vis sum frequency spectra were obtained by a home-built sum frequency spectrometer similar to the one described in detail by Krause and Daum.[23] Pulse energies of the incident beams were always limited to 100 μJ to avoid damage of the monolayer.[24] The spectral resolution of the incident beams was 2 cm^{-1} for the visible (532 nm) and 5 cm^{-1} for the IR beam. Pulse duration of both beams was about 40 ps and the pulse repetition rate was 20 Hz. Both input beams and the analyzed SFG beam were p-polarized. To minimize surface contamination during the measurements, the samples were mounted in a nitrogen-purged cell, which was covered by a CaF_2 window of 1-mm thickness. The angles of incidence were 50° for the visible and 60° for the IR beam with respect to the substrate normal. The IR beam was focused by a CaF_2 lens with a focal length of 300 mm yielding a beam diameter of about 1 mm at the surface, whereas the visible beam was about 3 mm in diameter and remained unfocused.

For data acquisition the laser system was tuned automatically within the entire range of the CH stretching vibrations. The step width was 2 cm^{-1}. For each data point 125 laser pulses were averaged. Usually two spectra were taken from each of three to four different locations of the sample surface and averaged after proper energy correction with respect to the energy variations of the IR beam. Finally, the averaged spectra were normalized to the nonresonant substrate signal at the lower energy end of the spectrum, that is, the region around 2750−2770 cm^{-1}. Since the nonresonant background is coverage dependent its change has to be taken into account if band intensities of a particular mode at different coverages are compared. The acquisition of several spectra was done for two reasons. First, it yields information about the uniformity of the film, e.g., about the quality of the sample, and second, this allows exclusion of any changes of the film during the time needed for the acquisition of the SFG spectrum. Particularly at incomplete thiol coverage we cannot assume a priori that the conformational state of the molecules is time independent.

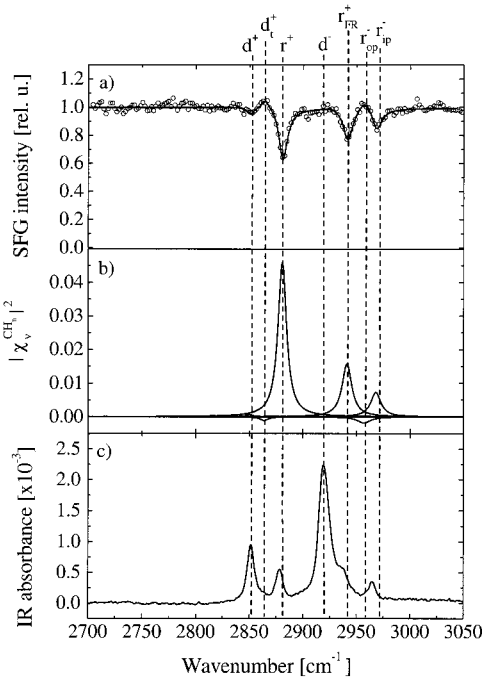

Figure 2. Decomposition of the C−H stretching region of an SFG spectrum of docosanethiol on polycrystalline gold (a) into Lorentz type resonances (b) and comparison with an IR-reflection absorption spectrum (c).

IV. Results and Analysis

Before turning to the kinetics of film formation we first present the spectrum of a completed monolayer (Figure 2) to demonstrate the evaluation procedure and to provide a comparison with conventional IRRAS. Furthermore, we briefly discuss how contaminations on the substrate interfere with the spectral features of the thiols and thus complicate data analysis in the initial stages of thiol adsorption.

Decomposition of SFG Spectra. The normalized SFG spectrum depicted in Figure 2a is analyzed according to eq 4. To fit the SFG spectra, two simplifying assumptions are made. First, all resonances are fit by Lorentzian line profiles. This is not necessarily an appropriate description, since the resonances could be inhomogeneously broadened. However, it turned out that the resonances are described well enough by Lorentzian lines, hence making more sophisticated fits using a superposition of Lorentzians and Gaussians superfluous. We note that the bandwidth of the laser system is not the reason, since it is significantly smaller than the width of the vibrational bands. The second assumption is that all resonances are in phase; that is all ϕ_v's are identical except for a phase shift of π to allow constructive or destructive interference. Strictly speaking this is incorrect. As mentioned above, the phase factors are affected by the orientation of the modes and, therefore, are expected to be different. However, since in this work we are interested in a qualitative interpretation of the temporal evolution of the SFG spectra, rather than extracting quantitative information about the orientation of molecular groups, we can adopt this simplified

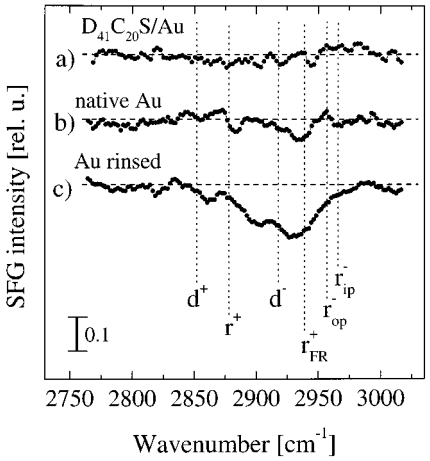

Figure 3. SFG spectra in the range of the C−H stretching vibrations for gold substrates which have been subjected to different treatments: (a) substrate coated with a SAM of perdeuterated eicosanethiol; (b) a freshly prepared Au substrate; (c) a freshly prepared Au substrate after rinsing with ethanol. Spectra are displaced for clarity. The unit bar indicates the intensity of the resonance relative to the nonresonant signal.

scheme by only using the intensities of the resonances to trace the formation of the thiol film. A constant phase of 1.735 ± 0.1465 was obtained for all fits. Furthermore, as shown elsewhere,[25] the error introduced this way is small for the system under consideration and, analogous to the empirical justification for using Lorentzian lines, a fit of the resonances with ϕ_v as a free parameter does not improve the quality of the fit. For the latter to become relevant the signal-to-noise ratio (S/N) has to be improved.

The resonances (eq 2) are shown separately in Figure 2b. For comparison with the IR spectrum the square of the susceptibility is displayed. Due to the coherent superposition of resonant signals with the nonresonant background, constructive and destructive interference occurs depending on the orientation of the molecular entity. For this reason the sign of the susceptibility has been maintained. The superposition of the resonant susceptibilities with the nonresonant background yields the solid line of Figure 2a. This coherence has been used earlier to infer the orientation of CH_3 groups.[26] As demonstrated, the fit is an excellent phenomenological description of the experimental data. For comparison, Figure 2c shows the IRRAS spectrum of an identical SAM of docosanethiol on gold. The dominant features are the symmetric and antisymmetric methylene vibrations at 2851 and 2919 cm^{-1}. In contrast, there is almost no intensity for the respective SFG resonances. This is due to the high degree of all-trans conformation of the hydrocarbon chains, which represent a centrosymmetric arrangement of the methylene groups. Note that in contrast to IR, SFG reveals two additional features, which both are opposite in sign. Even though they have low intensity, the bands around 2864 and 2956 cm^{-1} are significant and needed to describe the SFG spectrum appropriately. On the basis of SFG studies of the chain length dependence of thiol SAMs which clearly exhibit an odd−even effect,[25] we can assign the first feature to the CH_2 (tCH_2) adjacent to the methyl group. Very recently, this band has been identified as well in an SFG study of hydrocarbon-terminated ethylene glycols.[27] The second feature is identified with the antisymmetric out-of-plane CH_3 vibration and has been noticed before by Bain et al.[22] For the evaluation of the kinetics the intensities of the vibrational bands are evaluated at different stages of thiol adsorption.

Influence of Contaminations on the Evaluation of SFG Spectra. Figure 3 compares a SAM of perdeuterated eicosanethiol on gold with a Au substrate right after evaporation and with another Au substrate thoroughly rinsed with ethanol. As seen from the topmost spectrum a SAM of alkanethiol resists the adsorption of contaminants. The spectrum of the fresh gold substrate is still rather flat, even though spectral features have started to evolve. Pronounced changes occur if the sample is thoroughly rinsed with ethanol. Analogously, immersion of the samples causes the adsorption of impurities as well. This means that changes in vibrational spectra during the initial stages of thiol adsorption are not solely due to thiol molecules but impurities also contribute. However, around 2850 cm^{-1} the signal is small and changes in this range can be safely associated with the thiols. Since the effect of contaminations cannot be completely excluded, we minimize this effect by only using samples which were freshly evaporated. We note at this point that with respect to the detection of contaminants SFG has a significant advantage compared to IR since it does not require a reference spectrum. IR, which suffers from the low absorption, can produce easily distorted spectra if the reference is not free of contaminants.

Kinetics of Film Formation. The temporal evolution of the vibrational spectra was monitored by preparation of three completely independent series of Au samples with immersion times between 1.5 min and 48 h in 3 μM ethanolic solution. For the measurement of the change of the nonresonant background due to the thiolate formation (χ_{Au-S}) four different measurements were performed.

We first discuss the coverage dependence of the nonresonant background for two reasons. Firstly, the background is changed by the Au−S bond formation and thus serves as an indicator of the thiol coverage. Secondly, the quantitative evaluation normalizes the resonance intensities to that of the nonresonant background. Thus, its coverage dependence has to be known to get the absolute change of the resonance intensities. The alteration of the substrate signal by thiolate formation has been extensively used in studies of the adsorption kinetics of thiols by SHG.[3,4,12,28] For the wavelength used in these studies it turned out that χ_{Au-S} is proportional to the thiol coverage. Furthermore, its change is phenomenologically approximated by Langmuir kinetics, thus providing a simple measure of the thiol coverage. However, we cannot be sure a priori that the signal/coverage relationship is as simple at the SFG wavelength as it is for the case of SHG when using a fundamental wavelength of 1064 nm. As has been shown resonance effects can alter the shape of an adsorption curve dramatically thus making a quantitative evaluation complicated.[29] The equivalence of the nonresonant SFG signal and the SHG signal was tested by comparative SFG and SHG measurements. Freshly evaporated Au samples were mounted into a sample holder in such a way that the thiol coverage could be increased stepwise by immersion of the substrate into the 3 μM docosanethiolate solution for a certain period of time, then rinsed with ethanol and blown dry with nitrogen. For each immersion time, the signal was recorded at two different frequencies: above (3050 cm^{-1}) and below (2770 cm^{-1}) the range of the CH stretching vibrations. As suggested already by the equal signal levels of the spectra of Figure 3, the changes are identical at both frequencies. The coverage dependence of the nonresonant signal is shown in Figure 4. As can be seen the nonresonant substrate signal decreases quickly within the first 5 min of adsorption and then saturates at about 75% of the initial value of the bare gold substrate. The solid line represents a least-squares fit based on simple Langmuir

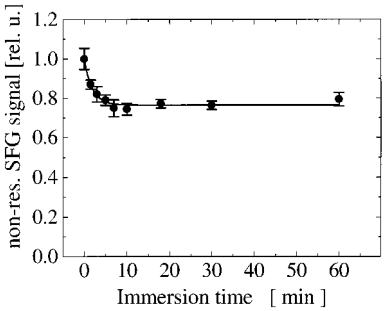

Figure 4. Dependence of the nonresonant SFG signal from a gold substrate on the time of immersion in a solution of docosanethiol in ethanol. The thiol concentration was 3 μM. The solid line is a fit based on eq 6. $k_{Au-S} = 2820$ L mol^{-1} s^{-1}.

kinetics:[4]

$$I_{SFG}^{NR} \propto |\chi_{Au} + \chi_{Au-S}(1 - e^{-k_{Au-S}t})|^2 \qquad (6)$$

Within the precision of about 10−15% we measured in the present incremental experiments, the rate constant of thiolate formation ($k_{Au-S} = 2820$ L/mol^{-1}) is in agreement with the value of about $k_{Au-S} = 2400$ L/mol^{-1} which was obtained from independent SHG experiments.[12] In these continuous in situ experiments the thiol adsorption was monitored in real time without disturbing the system. The agreement between the ex situ SFG and the in situ SHG measurements gives confidence to use the evolution of the nonresonant substrate signal as an indicator of surface coverage. We define the adsorption time at which the exponential of eq 6 has decayed to 0.1 as the boundary between the initial step of film formation where most of the thiol molecules adsorb and the subsequent steps which produce the complete monolayer. As reported elsewhere the thiol coverage amounts to 80−90% after this fast, initial adsorption step.[1,2,8]

The time evolution of the SFG spectra of docosanethiol on gold is shown in Figure 5. In this selection of SFG spectra Au samples were immersed in a 3 μM solution of docosanethiol in ethanol for different periods of time ranging from 1.5 min to 48 h. For clarity the spectra have been displaced. Since the nonresonant background is coverage dependent (see Figure 4), the spectra are scaled such that the intensities of vibrational bands at different immersion times can be compared directly. The intensity of the resonances relative to the nonresonant signal at zero coverage is inferred from the unit bar. The shadowed regions mark the locations of the various CH-stretching vibrations as listed in Table 1.

Starting from the structureless spectrum of the native substrate, pronounced vibrational features evolve and change fundamentally with progressing adsorption time. Up to immersion times of 5 min, the spectra are dominated by two broad features peaking around 2916 and 2813 cm^{-1}, respectively. The feature labeled "c_s" around 2813 cm^{-1} is unexpected and will be discussed in more detail below. The spectral feature at 2916 cm^{-1} is a clear signature of the methylene group and indicates a high degree of gauche conformations in the hydrocarbon chains. This causes the methyl end groups to be randomly oriented and, consequently, they do not give rise to an SFG signal. At 1.5 min the spectral features are very broad, and only for $t > 3$ min the methylene mode at 2916 cm^{-1} starts to rise above the average level. The close similarity to the spectrum shown in Figure 3 strongly suggests that the signals do not originate solely from thiols but originate also from contaminants and possibly incorporated solvent. At immersion times of about

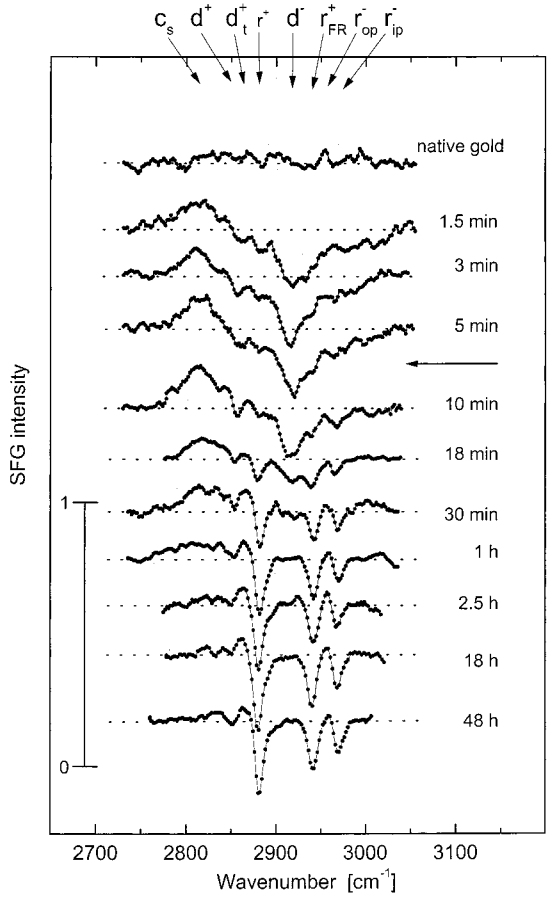

Figure 5. Adsorption of docosanethiol on gold from a 3 μM solution in ethanol. Time evolution of the SFG spectrum in the range of the C−H stretching vibrations. The bars mark the different modes compiled in Table 1. The spectra are labeled by immersion times and are displaced for clarity. The intensity of the resonances relative to the nonresonant signal at zero coverage can be inferred from the unit bar. The horizontal arrow between 5 and 7 min indicates the completion of the initial fast step, i.e., at this point the coverage is about 0.8−0.9.

TABLE 1: Assignment of C−H Stretching Vibrations

description	symbol	wavenumber, cm^{-1}
CH_3, antisymmetric in-plane	r^-_{ip}	2968
CH_3, antisymmetric out-of-plane	r^-_{op}	2954
CH_3, sym Fermi	r^+_{FR}	2940
CH_3, sym	r^+	2880
CH_2, antisym	d^-	2916
tCH_2, sym, adjacent to CH_3	d_t^+	2864
CH_2, sym	d^+	2855
soft mode	c_s	2813

5 min the increase of the coverage is already slowing down significantly (see Figure 4). Nevertheless, the dominating CH_2 signal reveals that the chains are still strongly kinked. For $t >$ 5 min the spectral features begin to sharpen and at the same time the methyl groups appear. This indicates that the molecules other than thiols are displaced and that the conformation of the chains is changing. This progression of ordering is clearly seen beyond 10 min immersion time where the methylene mode at 2916 cm^{-1} loses and the methyl modes gain intensity. The final spectrum is completely dominated by the methyl modes and thus indicates a high degree of order in the completed monolayer.

In contrast to all other spectral features the band centered at 2813 cm^{-1} does not correspond to any C−H stretching vibration of a free molecule. Like the methylene signal it is transient and occurs only at incomplete thiol coverage. As demonstrated by

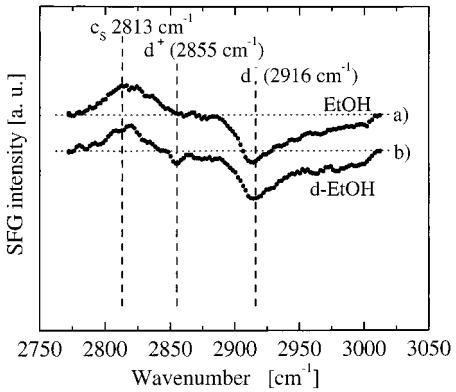

Figure 6. SFG spectra of an incomplete layer of docosanethiol on gold: (a) adsorption from normal ethanol and (b) from perdeuterated ethanol. The thiol concentration was 3 μmol/L and the immersion time was 7 min.

Figure 6, which shows a comparison of thiol adsorption from normal and perdeuterated ethanol, this is due to the thiol itself and not due to solvent molecules which might be trapped in the incomplete thiol layer. Docosanethiol adsorbed from ethanol or perdeuterated ethanol yields identical results. At present the details of this structure are not completely clear, but a mode softening caused by the interaction of the thiol with the metal substrate is most likely. The appearance of modes atypical for the free molecule has been reported in a number of ultrahigh vacuum studies of linear and cyclic alkanes on different metals.[30−33] In particular, the recent work of Yamamoto et al.[30] strongly favors this interpretation, since they also observed a band around 2815 cm^{-1} in an IRRAS study of tetratetracontane (n-$C_{44}H_{90}$) on Au(111) and Ag(111). For alkanethiols this effect should be most pronounced at low coverage where the alkane chains can orient themselves parallel to the substrate and form a "striped phase".[10,17] Similar to the UHV experiments on the hydrocarbon[30−33] the bandwidth of the soft mode observed in our experiments is also larger (25−40 cm^{-1}) compared to that of normal vibrations (∼12−15 cm^{-1}). Several factors are likely to contribute. Besides different groups, i.e., methyl and methylene, interact with the surface both damping and inhomogeneous broadening can account for the broadening. The relative importance of the different effects is not clear at present and further investigations are needed to pinpoint the details.

The qualitative picture of the temporal evolution of the C−H vibrations obtained from the spectra of Figure 5 can be detailed by quantifying the resonance intensities according to the procedure outlined in section II (eq 5). The result is summarized in Figure 7. Since the resonance intensities are normalized to the coverage-dependent nonresonant substrate signal they were corrected according to the coverage-dependent change of the nonresonant substrate signal as displayed in Figure 4. Note the logarithmic scale of the immersion time. As discussed above contaminants and/or solvent molecules can give rise to vibrational features as well. For this reason we have included the horizontal dotted lines in each of the eight graphs which indicate the intensities of the respective resonances obtained for samples which were immersed into pure solvent. Therefore, these lines mark the upper limit of the solvent-based background. Even though this contribution can be significant, the levels are much lower than the variations of the intensities of the thiol vibrations. Thus, we can safely neglect the contribution from this background in the discussion of time scales.

To characterize the process of film formation, we fit the data

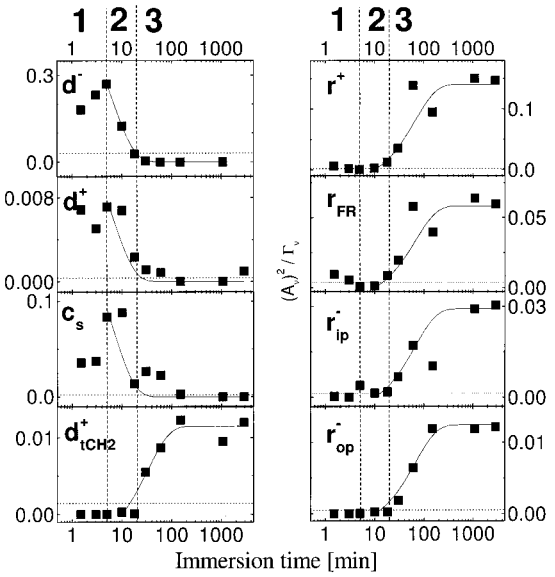

Figure 7. Time evolution of the intensity of the vibrational modes of docosanethiol. Experimental conditions are identical to those of Figure 5. The solid lines are based on eqs 7 and 8, with the values of k_ν and $t_{\nu,0}$ compiled in Table 2. The vertical dotted lines characterize the sequence of steps. The values of 5 and 20 min result from the decrease of the exponentials of eqs 6 and 7 to a value of 0.1. The bar at 20 min results from the delay time of 5 min and the decay time of 15 min.

TABLE 2: Time Constants and Delay Times for the Change of Intensity of the C−H Stretching Modes during Thiol Film Formation

mode ν	symbol	$t_{\nu,0}$, s	$k_{\nu/\mathrm{Au-S}}$, L mol^{-1} s^{-1}	$k_{\nu,\mathrm{rel}}$
Au−S	nr	0	2800	1
CH_2, antisym	d^-	300	830	0.3
CH_2, sym	d^+	300	830	0.3
soft mode	c_s	300	830	0.3
t-CH_2, sym, adjacent to CH_3	d_t^+	600	170	0.06
CH_3, antisymmetric out of plane	r^-_{op}	600	80	0.029
CH_3, antisymmetric in plane	r^-_{ip}	600	80	0.029
CH_3, sym	r^+	600	80	0.029
CH_3, sym, Fermi	r_{FR}^+	600	80	0.029

of Figure 7 to the following phenomenological expressions

$$I_\nu = I_0 + I_{\max} e^{-k_\nu (t - t_{\nu,0})} \qquad t \geq t_{\nu,0} \tag{7}$$

for decreasing and

$$I_\nu = I_0 + I_{\max}(1 - e^{-k_\nu (t - t_{\nu,0})}) \qquad t \geq t_{\nu,0} \tag{8}$$

for increasing intensities. k_ν reflects the rate by which mode ν changes and $t_{\nu,0}$ is the time delay with respect to the beginning of thiol adsorption. $I_{\max}$ denotes the initial and final band intensity, respectively. Figure 7 shows the temporal evolution of the band intensities and the corresponding curves based on eqs 7 and 8. The values of k_ν and $t_{\nu,0}$ are compiled in Table 2. It is obvious from Figure 7 that we can distinguish three time scales which are characterized by the change of the nonresonant background, the methylene modes, and the methyl modes. The vertical dotted lines, which are given by the decrease of the exponentials of eqs 6 and 7 to a value of 0.1, indicate the different steps involved in the film formation.

The initial stage is characterized by the Au−S bond formation (Figure 4) and extends over the first 5−6 min at the concentration used in our experiments. During this period of time thiols adsorb up to a coverage of about 80−90% of a monolayer[1,2,8] and cause the nonresonant signal to decrease. The increase in

thiol coverage is reflected as well by the increase of the signals from the asymmetric methylene mode and the soft mode.

The pronounced decrease of the intensity of the asymmetric CH_2 band determines the second step. The decline of this signal to noise level proceeds about 3−4 times more slowly than the first step. This clearly indicates a transition of the hydrocarbon chains from a highly kinked state to the all-trans conformation. In principle, an orientation of the IR transition dipole moment parallel to the substrate would also explain such a behavior. However, IR measurements yield a continuously increasing intensity and thus rule out this explanation. Furthermore, the symmetric methylene mode behaves analogously, as expected. Additional evidence for the establishment of molecular order comes from the intensity of the "soft mode" at 2813 cm^{-1}. It exhibits the same temporal evolution and thus indicates the loss of interaction of the hydrocarbon chains with the substrate due to the increasing thiol density.

The third time scale on which changes of the methyl resonances occur (see right half of Figure 7) is significantly delayed (20 min in the present study). Furthermore, the rate is lower by a factor of at least 35 compared to the initial step. Since, as outlined in section II, SFG is symmetry sensitive, the pronounced increase of the methyl mode intensities reflect the transition from an essentially amorphous arrangement to a structure with the methyl groups aligned. Parallel to this reorientation, we observe an increase of the intensity associated with the terminal methylene group. Its temporal behavior is remarkably opposite to that of the rest of the methylene modes.

V. Discussion

Summarizing the results of the previous section, three rather different times scales are identified by the evolution of the SFG spectra. Every time scale can be associated with a particular part of the substrate-adsorbate system. The Au−S bond formation which starts immediately after immersing the substrate into the thiol solution is followed by a straightening of the alkyl chains after a significant time delay. The decrease of the methylene mode intensity clearly indicates the establishment of a relatively well ordered layer within a rather short time. However, the reorientation of the methyl and terminal methylene groups on a much longer time scale suggests that order formation progresses from the interface to the upper part of the layer.

The rather slow rate of completion of the monolayer raises the question, what causes final ordering. SFG on incomplete layers suggests that adsorption of the last few percent of thiol molecules induces the ordering and alignment of the terminal methyl groups. According to ellipsometric measurements[1] and plasmon resonance spectroscopy,[8] which after the fast initial step see a slow increase of the film thickness up to the final value, the last 10−20% percent of the thiol molecules adsorbing seem to induce the order. Preparing a sample which still shows the modes indicative of a disordered layer, e.g., c_s and d^-, and immersing it in pure ethanol does not produce any intensity of the methyl modes.[34] If ordering occurred, islands with oriented methyl moieties should form. We note that XPS did not show a substantial desorption of thiol molecules when immersed in pure solvent for 20 h. Schlenoff et al. reported a loss of about 25% for octadecanethiol in ethanol.[35] The origin of this difference is not clear but the longer chain length used in our experiment might account for it.

We would like to close the analysis of the temporal evolution of order in the SAM with a discussion of the precision of the rate constants given above. The error in the initial rate constant determined via the nonresonant background is less than 15%. Considering the in situ SHG experiments it can even be reduced to about 5%.[12] In contrast, the uncertainty for the other rate constants is much higher and the values extracted from the temporal evolution of the vibrational resonances are only reliable within a factor of 2. The reason for the significantly lower precision is 2-fold. First, the vibrational bands overlap and even might interfere destructively. With the given signal/noise ratio there is some freedom in fitting the resonances. This is particularly true since we merely measure the intensity of the SFG signal and have no information about the phase of the signal. This point becomes particularly severe for bands with low intensity, e.g., the d^+ or the d^+_t modes. Second, we observed certain variations of the band intensities for different series of adsorption experiments. Despite the fact that we took great care to minimize the influence of poorly controllable factors such as impurities by always using freshly evaporated substrates and measuring the samples under inert gas atmosphere, we could not completely avoid short time exposure to the ambient. Considering that incomplete films can still adsorb impurities it is easy to imagine that the quality of the film and, thus, the intensity of the resonances are affected to some extent. Related to this issue is the question whether the ex situ measurements represent the real situation, i.e., the film in contact with the solvent.[36] In general, solvent molecules are incorporated into the incomplete film and, therefore, the degree of gauche conformations is likely to be different from that of a film in contact with a gas atmosphere. This could somewhat affect the intensities of the vibrational bands, even though it will not alter their general temporal evolution. With these limitations in mind it does not make sense to discuss differences in rate constants such as those between the terminal methylene group and the methyl modes shown in Figure 7.

How do the three steps of film formation relate to previous work? A two-step mechanism has been reported in the early study of Bain et al.[1] Subsequent investigations of the kinetics of film formation by NEXAFS,[2] IR,[6] and surface plasmon spectroscopy (SPS)[8] confirmed this result. The ratio of the rate constants of the first, fast step which reflects the Au−S bond formation and of the third step involving the reorientation of the methyl groups agrees with the SPS work of deBono et al.[8] They identified a factor of 100 between the first and a second step, which in their case was found to lead to the final film thickness. In the IR study of Truong and Rowntree[6] on butanethiol on gold also different time scales were identified. Even though no detailed rate constants were provided, the time scales seem consistent with our values. The vibrational spectrum revealed a first step, characterized by a substantial decrease of methylene features, and a pronounced increase of methylene bands. A second slow step is inferred from changes in the intensities of the methyl bands. However, these changes are very small and barely above the experimental uncertainty. With respect to the changes in orientation, SFG as a nonlinear technique has the advantage of higher sensitivity compared to IR. Whereas the IR intensity varies with the $\cos^2$ of the angle between the transition dipole moment and the surface normal, SFG in a first approximation varies with $\cos^6$. In another kinetic study, Bensebaa et al.[7] investigated docosanethiol on gold also with IR. Unlike butanethiol,[6] the final spectrum is dominated by the methylene modes. In contrast to our findings with the same molecule, they did not observe distinctly different steps. At comparable concentrations an ordered monolayer is reported to form within 45 s, which is, depending on the definition of

ordered, 1−2 orders of magnitude faster than our rates. Only slight changes such as a small shift of r^--bands are detected at longer times. The authors exclude any major changes in coverage after 45 s. The origin of this discrepancy with other work which reports a further increase in film thickness after the initial fast phase[1,2,8] is not clear. Closing the comparison of the SFG data with the kinetic studies by IR, we note that the vibrational band at $\sim$2813 cm^{-1} has not been reported before for butanethiol or for docosanethiol.

Whereas the rate of film formation in the IR studies just discussed is much higher, NEXAFS data[2] show a time scale for ordering somewhat extended with respect to the present SFG results. The most likely explanation is that in these early experiments the quality of the substrate, i.e., the level of contaminations, was not explicitly controlled. However, this can significantly affect the rate constants and can slow the rate of film formation. We think this to be the reason, rather than the difference in the techniques, i.e., sensitivity to different aspects of the system.

Finally we compare thiol film formation from solution with that from the gas phase under UHV conditions. Both preparation procedures reveal a stepwise process and a three-step process is found both with SFG and with UHV techniques. In the UHV study by Schreiber et al.[15] a phase of flat lying molecules ("striped phase") forms first for $\theta < 0.27$, followed by an intermediate phase of unknown structure above $\theta = 0.27$ and the onset of the final c(4 × 2) phase above $\theta = 0.47$. Taking the soft mode as an indicator of the flat lying molecules growth from solution also produces such a phase, which gradually decreases with increasing coverage. However, for solution-grown films there are no clear hints that an ordered striped phase is formed. Due to the presence of the solvent the formation of such a phase might be either thermodynamically or kinetically hindered. The situation in solution is probably better imagined by chemisorbed molecules interacting with the surface via part of the hydrocarbon chain. Furthermore, this situation is expected to be dynamic rather than static; i.e., the contact of the chain with the surface competes with the solvent−substrate interaction. Even though the STM work of Yamada and Uosaki[10] is not directly comparable since decanethiol ($H_{21}C_{10}SH$) and a different solvent were used, it suggests a kinetic phenomenon. At low coverage they identified a striped phase, whereas at concentrations comparable to the ones used in our experiments, no striped phase was observed. In our case the soft mode persists up to rather long immersion times $\leq$60 min. This indicates that even at high coverage (>80%) the hydrocarbon chains have substantial contact with the substrate. Unfortunaly, we cannot draw any conclusions on the number of interaction from the intensity since the susceptibility tensor (eq 2) is dependent not only on the coverage but also on the orientation of the molecular moieties.

Even though there is agreement between the UHV and solution experiments with respect to the number of steps, two major differences exist. The first one is the significantly smaller ratio (1/500) of the time constants of the first and last step in the UHV experiments compared to our results ($\sim$1/50). The second is that an ordered phase is observed at coverages significantly lower than in solution as indicated by the appearance of methyl modes. This suggests that even though it seems that there is a general mechanism for the formation of alkanethiol layers, the details are dependent on the preparation condition, i.e., preparation by sublimation or from a solvent. That also the kind of solvent is critical has been demonstrated by SHG experiments of an end group modified thiol where the change of solvent alters the sequence of adsorption and reorientation dramatically.[28]

VI. Conclusion

Not only being sensitive to thiolate formation but also being specific to the conformational changes and orientation of submolecular entities, IR−vis SFG provides a detailed picture of the process of film formation. For docosanethiol adsorbed from ethanol, a three-step process is identified. Even though the mechanism deduced exhibits a parallelism to the UHV adsorption studies, there are significant differences which arise from the presence of the solvent. Since, in general, the system is determined by a complex interplay of interactions between the SAM molecules, the substrate, and the solvent, it is not surprising that the actual mechanism strongly depends on the details of the system. Studies using different solvents and substrates are under way to elucidate this point.

Acknowledgment. Support by the Deutsche Forschungsgemeinschaft and the Fonds der Chemischen Industrie is gratefully acknowledged. We thank R. Kohring and A. Lampert for developing the data evaluation software, G. Albert for the substrate preparation, J. Pipper for the synthesis of the deuterated thiol, and O. Dannenberger for comparative SHG measurements and the synthesis of the docosanethiol.

References and Notes

(1) Bain, C. D.; Troughton, E. B.; Tao, Y.-T.; Evall, J.; Whitesides, G. M.; Nuzzo, R. G. *J. Am. Chem. Soc.* **1989**, *111*, 321.
(2) Hähner, G.; Wöll, C.; Buck, M.; Grunze, M. *Langmuir* **1993**, *9*, 1955.
(3) Buck, M.; Eisert, F.; Fischer, J.; Grunze, M.; Träger, F. *Appl. Phys. A* **1991**, *53*, 552.
(4) Buck, M.; Eisert, F.; Fischer, J.; Grunze, M.; Träger, F. *J. Vac. Sci. Technol. A* **1992**, *10*, 926.
(5) Karpovich, D. S.; Blanchard, G. J. *Langmuir* **1994**, *10*, 3315.
(6) Truong, K. D.; Rowntree, P. A. *Prog. Surf. Sci.* **1995**, *50*, 207.
(7) Bensebaa, F.; Voicu, R.; Huron, L.; Ellis, T. H.; Ktuus, E. *Langmuir* **1997**, *13*, 5335.
(8) DeBono, R. F.; Loucks, G. D.; DellaManna, D.; Krull, U. J. *Can. J. Chem.* **1996**, *74*, 677.
(9) Peterlinz, K. A.; Georgiadis, R. *Langmuir* **1996**, *12*, 4731.
(10) Yamada, R.; Uosaki, K. *Langmuir* **1997**, *13*, 5218.
(11) Tamada, K.; Hara, M.; Sasabe, H.; Knoll, W. *Langmuir* **1997**, *13*, 1558.
(12) Dannenberger, O.; Buck, M.; Grunze, M. *J. Phys. Chem. B* **1999**, *103*, 2202.
(13) Balzer, F.; Gerlach, R.; Polanski, G.; Rubahn, H. G. *Chem. Phys. Lett.* **1997**, *274*, 145.
(14) Gerlach, R.; Polanski, G.; Rubahn, H. G. *Appl. Phys. A* **1997**, *65*, 375.
(15) Schreiber, F.; Eberhardt, A.; Leung, T. Y. B.; Schwartz, P.; Wetterer, S. M.; Lavrich, D. J.; Berman, L.; Fenter, P.; Eisenberger, P.; Scoles, G. *Phys. Rev. B* **1998**, *57*, 12476.
(16) Fenter, P.; Schreiber, F.; Berman, L.; Scoles, G.; Eisenberger, P.; Bedzyk, M. J. *Surf. Sci.* **1998**, *412−413*, 213.
(17) Poirier, G. E.; Tarlov, M. J.; Rushmeier, H. E. *Langmuir* **1994**, *10*, 3383.
(18) Bain, C. D. *J. Chem. Soc., Faraday Trans.* **1995**, *91*, 1281.
(19) Hines, M. A.; Todd, J. A.; Guyot-Sionnest, P. *Langmuir* **1995**, *11*, 493.
(20) Miranda, P. B.; Pflumio, V.; Saijo, H.; Shen, Y. R. *Chem. Phys. Lett.* **1997**, *264*, 387.
(21) Shen, Y. R. *The Principles of Nonlinear Optics*; John Wiley & Sons: New York, 1984.
(22) Bain, C. D.; Davies, P. B.; Ong, T. H.; Ward, R. N.; Brown, M. A. *Langmuir* **1991**, *7*, 1563.
(23) Krause, H.-J.; Daum, W. *Appl. Phys. B* **1993**, *56*, 8.
(24) Goto, Y.; Akamatsu, N.; Domen, K.; Hirose, C. *J. Phys. Chem.* **1995**, *99*, 9, 4086.
(25) Lampert, A.; Eisert, F.; Buck, M.; Grunze, M., in preparation.
(26) Ward, R. N.; Davies, P. B.; Bain, C. D. *J. Phys. Chem.* **1993**, *97*, 7141.
(27) Goates, S. R.; Schofield, D. A.; Bain, C. D. *Langmuir* **1999**, *15*, 1400.

(28) Dannenberger, O.; Wolff, J. J.; Buck, M. *Langmuir* **1998**, *14*, 4679.
(29) Buck, M.; Eisert, F.; Grunze, M.; Träger, F. *Appl. Phys. A* **1995**, *60*, 1.
(30) Yamamoto, M.; Sakurai, Y.; Hosoi, Y.; Ishii, H.; Ito, E.; Kajikawa, K.; Ouchi, Y.; Seki, K. *Surf. Sci.* **1999**, *427/428*, 388.
(31) Manner, W. L.; Bishop, A. R.; Girolami, G. S.; Nuzzo, R. G. *J. Phys. Chem. B* **1998**, *102*, 8816.
(32) Raval, R.; Chesters, M. A. *Surf. Sci.* **1989**, *219*, L505.
(33) Witte, G.; Weiss, K.; Jakob, P.; Braun, J.; Kostov, K. L.; Wöll, C. *Phys. Rev. Lett.* **1998**, *80*, 121.
(34) Himmelhaus, M. Ph.D. Thesis, 1997.
(35) Schlenoff, J. B.; Li, M.; Ly, H. *J. Am. Chem. Soc.* **1995**, *117*, 12528.
(36) Since ethanol strongly absorbs in the wavelength range investigated here, no in situ studies were feasible.